Geomechanics and Engineering, *Vol. 24, No. 6 (2021) 519-529*
DOI: https://doi.org/10.12989/gae.2021.24.6.519

Deformation and permeability evolution of coal during axial stress cyclic loading and unloading: An experimental study

Kai Wang[1,2], Yangyang Guo*[1,2,3], Hao Xu[1,2], Huzi Dong[1,2], Feng Du[1,2] and Qiming Huang[3]

[1]*School of Emergency Management and Safety Engineering, China University of Mining & Technology (Beijing), Beijing 100083, China*
[2]*Beijing Key Laboratory for Precise Mining of Intergrown Energy and Resources, China University of Mining & Technology (Beijing), Beijing 100083, China*
[3]*Key Laboratory of Mine Disaster Prevention and Control, Shandong University of Science & Technology, Qingdao, 266590, China*

(Received September 23, 2020, Revised March 8, 2021, Accepted March 15, 2021)

Abstract. In coal mining activities, the abutment stress of the coal has to undergo cyclic loading and unloading, affecting the strength and seepage characteristics of coal; additionally, it can cause dynamic disasters, posing a major challenge for the safety of coal mine production. To improve the understanding of the dynamic disaster mechanism of gas outburst and rock burst coupling, triaxial devices are applied to axial pressure cyclic loading-unloading tests under different axial stress peaks and different pore pressures. The existing empirical formula is use to perform a non-linear regression fitting on the relationship between stress and permeability, and the damage rate of permeability is introduced to analyze the change in permeability. The results show that the permeability curve obtained had "memory", and the peak stress was lower than the conventional loading path. The permeability curve and the volume strain curve show a clear symmetrical relationship, being the former in the form of a negative power function. Owing to the influence of irreversible deformation, the permeability difference and the damage of permeability mainly occur in the initial stage of loading-unloading, and both decrease as the number of cycles of loading-unloading increase. At the end of the first cycle and the second cycle, the permeability decreased in the range of 5.777 - 8.421 % and 4.311-8.713 %, respectively. The permeability decreases with an increase in the axial stress peak, and the damage rate shows the opposite trend. Under the same conditions, the permeability of methane is always lower than that of helium, and it shows a V-shape change trend with increasing methane pressures, and the permeability of the specimen was 3 MPa > 1 MPa > 2 MPa.

Keywords: cyclic loading- unloading; axial stress; gas pressure; deformation; permeability damage rate

1. Introduction

The coal seam is a typical porous medium. Whether it is mine disaster prevention or exploitation and utilization of CBM, the relationship between coal/rock deformation and gas seepage is required (Lama *et al*. 2002, Rudakov and Sobolev *et al.* 2019, Sobczyk 2011, 2014, Jorat *et al*. 2013). During the processes of coal mining, drilling, and blasting, the stress field of the coal seams in front of the working face are repeatedly under the influence of periodic weighting. Afterward, it causes a dynamic change in the coal seam in front of the working face in the pressurization zone or the pressure relief zone. The abutment stress on the coal seam always undergoes a cyclic loading-unloading process (Li *et al.* 2018, Martin *et al.* 2003, Zhang *et al.* 2017, Wu *et al.* 2020). In contrast to the static stress state, under cyclic stress, the mechanical properties of coal seams and the pore-fracture structure contained in them change. Concurrently, changes in gas content and pressure during the mining process will also affect permeability to a certain extent, which may lead to dynamic disasters such as coal and gas outbursts or ground pressure impacts, threatening coal mining safety (Wang *et al.* 2012, 2019).

Recently, triaxial loading experiments have been performed to evolve the characteristics of coal samples, such as strength, strain, damage, and modulus of coal and rock during cyclic loading-unloading from experimental variables such as loading speed, number of cycles, and stress amplitude. For example, Chen *et al*. (2007) experimentally studied the strength and elastic properties of sandstone under different test conditions. They found that the unloading or reloading modulus under cyclic loading was greater than the loading modulus under monotonic loading. Jafari *et al* (2004) experimentally observed the behavior of rock joints under dynamic and cyclic loads. The results show that the shear strength of thin fractures increases with increasing confining pressure. Xu *et al* (2012) tested different rock materials and found that the unloading-loading curve form a closed plastic hysteresis loop. A negative exponential relationship between the residual strain and the number of cycles conforms. In Xie *et al*.'s (2020) study, coal samples were mechanically prefractured, and the complexity of the prefractured structures was described quantitatively.

The cyclic loading and unloading process is one of the main factors determining the mechanical properties of inelastic materials, which will cause local fractures to

*Corresponding author, Ph.D.
E-mail: doubleYGuo@163.com

ISSN: 2005-307X (Print), 2092-6219 (Online)

expand/close and then affect the permeability of coal/rock (Ghabezloo *et al.* 2009, Russell *et al.* 2004, Elsworth *et al.* 2012, 2013, Kasani *et al.* 2017). Fuenkajorn and Phueakphum (2010) studied the effects of cyclic loading on the uniaxial compressive strength, elastic modulus, and irreversible deformation of salt rock. Araei *et al* (2012) investigated the effects of initial stress states and loading rates on the stress–strain curves of rocks under uniaxial cyclic loading. Gordon *et al.* (1968) first reported the hysteresis of saturated rock under cyclic loading in 1968. Taheri *et al.* (2017) proposed and discussed an extensive test study on the mechanical properties of sandstone, and found that in the cyclic damage test, the amount of accumulated axial and transverse strains during the cyclic damage test was much greater than that in the cyclic hardening test. Fan and Liu (2019) injected adsorption/non-adsorption porous media and studied the variation in permeability. Many existing studies are based on the elastoplastic constitutive relationship, and much research has been conducted on the permeability change characteristics of different types of coal samples under loading and unloading. Miao *et al*. (2021) taking granite in Beishan of Gansu Province as the research object, triaxial cyclic loading and unloading tests were carried out. The evolution characteristics of energy dissipation, friction energy dissipation and breakage energy dissipation of rock under cyclic loading and unloading were explored. Wang *et al*. (2021) found compared with the uniaxial compression test, cyclic loading and unloading had a certain strengthening effect on the strength of the samples. The plastic deformation of the rock samples increased as the number of cycles increased. Jiang *et al*. (2021) performed constant amplitude cyclic loading and unloading tests on quasi-uranium ore to measure the degree of damage and used the closed chamber method to measure the accumulated radon concentration.

However, the permeability damage caused by the loading-unloading path has not been extensively studied i.e., the above studies have essentially ignored the influence of irreversible deformation on permeability, but it has a significant impact on the flow of gas in coal. In general, the combined effects of elastic strain, newly generated fractures, irreversible pore fracture closures, and fluid dissipation will affect the permeability and mechanical properties of coal. However, the axial pressure loading and unloading path of the induced permeability evolution remains largely unknown.

Because of this, this study investigates the deformation characteristics of coal samples under axial pressure cycling loading and unloading paths, and the evolution law of coal sample permeability under experimental conditions such as peak axial pressure, pore pressure, and different pore gases through laboratory tests. The effects of cyclic loading-unloading paths on the evolution of coal permeability were quantified through experiments. In addition, by comparing the experimental permeability of helium and gas, the effect of adsorption/desorption on the damage of coal permeability was studied. The permeability response in the process of cyclic loading and unloading is discussed to help the research on the mechanism of dynamic disaster prevention and provide a reference for the safe and efficient production of coal mine.

2. Experimental work

2.1 Experimental apparatus

This experiment uses a fluid-solid coupling triaxial device, which is mainly composed of a loading system, strain measurement system, gas supply system, constant temperature water bath system, flow meter, and data monitoring and control system, as shown in Fig. 1. The system can apply a maximum axial pressure σ_1 (large principal stress) of 70 MPa, maximum lateral pressure σ_2 (medium principal stress) of 35 MPa, maximum lateral pressure σ_3 (small principal stress) of 10 MPa, maximum gas pressure of 6 MPa, maximum axial displacement of 50 mm, and a maximum lateral displacement (single side) of 30 mm.

2.2 Specimen procurement and preparation

The strength of coal seams with a tendency to outburst (especially the soft stratification of coal seams) is usually very low, and direct drilling cannot be used to obtain test coal samples. Elsworth *et al.* (2013) discussed the deformation and strength characteristics of raw coal and briquettes. The research results show that the deformation characteristics and pore structure change rules of briquettes and raw coal with a certain particle size are identical; additionally, the results show that briquettes have the characteristics of easy processing, easy transportation, and artificial adjustment of molding parameters. Therefore, various pressure briquettes are often used as raw coal substitutes for use in the laboratory (Wang *et al.* 2013).

The pulverized was placed into the coal sample to form a mold and pressed to form 100×100×200 mm cuboid briquettes. To ensure that all the seepage gas passed only through the cross-section of the coal, the side of the coal was evenly coated with a layer of 704 silica gel with appropriate thickness and was sealed with a heat-shrinkable tube. The influence of the heat-shrinkable tube and the silicone on the experimental parameter collection can be ignored. While ensuring the tightness of the test unit, it does not affect the experimental results.

2.3 Experimental methods

This experiment used 99% high-purity methane, and the initial confining pressure was set to 4 MPa. The specimens were press-loaded and unloaded according to different paths. Among them, nine sets of specimens were tested, corresponding to nine different experimental conditions, each of which used two coal samples for experiments. From each set of data, a test piece with obvious regularity and data curve not affected by obvious external factors was selected, and then the corresponding comparative analysis was performed to obtain the deformation, failure, and seepage characteristics of the coal.

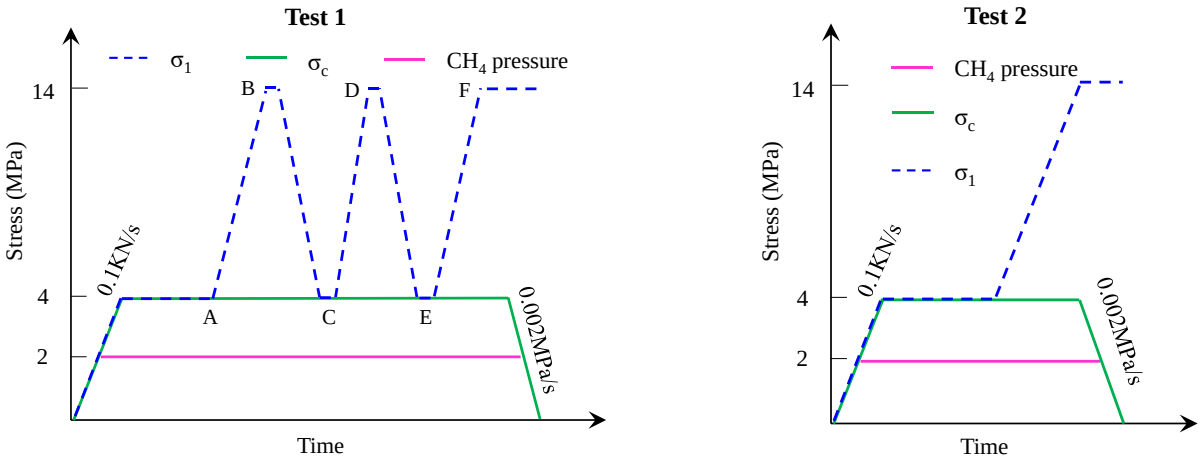

(a) Test 1 (b) Test 2

Fig. 2 Experimental path of cyclic axial stress loading-unloading and conventional axial stress

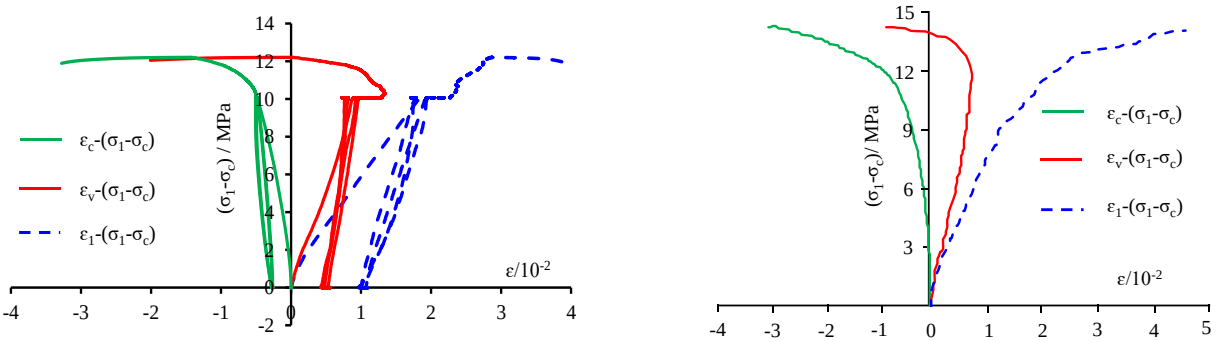

(a) Test1 (b) Test 2

Fig. 3 Strain–principal stress difference curves of Tests 1 and 2

3. Result and analyses

3.1 Deformation due to axial stress cyclic loading-unloading

To study the particularity of coal deformation during cyclic loading-unloading, an experimental scheme (Test 1) for cyclic loading-unloading of axial compression is shown in Fig. 2(a). First, the axial and confining stresses were loaded to 4 MPa hydrostatic conditions and simultaneously charged with methane at 2 MPa. Moreover, constant pressure adsorption was carried out for 24 h to bring the specimen to adsorption equilibrium (Because the coal sample is in the dynamic equilibrium state of adsorption-desorption during the test. In this test, the volumetric strain of coal sample is within 0.5%, that is, the coal sample has reach the adsorption equilibrium (Gang *et al.* 2019b)). Afterward, the axial stress was loaded at a speed of 0.1 KN/s at 14 MPa constant stress for 5 min and the axial stress was loaded to 4 MPa at a speed of 0.002 MPa/s. This cycle was repeated 2.5 times, and the axial stress was maintained. The confining stress was unloaded at a speed of 0.002 MPa/s until specimen failure. The axial stress unidirectional loading test (Test 2) was set for comparison, as shown in Fig. 2(b)). For the convenience of describing the experimental phenomenon using σ_1, σ_c represents the axis stress and the confining pressure; moreover, ε_1 and ε_c represent the axial and lateral strain, respectively.

Fig. 3 shows the strain–principal stress difference curves of Tests 1 and 2. Notably, there is a difference in deformation between both. Fig. 3(a)) shows that the cyclic loading-unloading process of the specimen (Test 1) has gone through the initial compaction, elastic, yield, and post-peak stages. After the coal completes the compaction phase, the axial stress received is less than the yield stress; therefore, the coal deformation is in the elastic phase, and the volumetric strain value is always greater than zero, i.e., coal undergoes shrinkage deformation. It can also be seen that the coal samples have good loading "memory". When the coal sample completes cyclic loading-unloading at one stage and enters the next stage, it is found that the axial strain-principal stress difference curve has the same shape as the original curve, but it will not completely coincide. Moreover, each loading and unloading will produce a hysteresis loop, indicating that during the process, the coal will suffer partial plastic damage. After the axial pressure loading and unloading is completed, the confining stress is unloaded. When the confining stress is reduced to a certain value, σ_1 reaches the yield stress, and the strain rate of the coal increases sharply, and damage occurs.

Fig. 3 shows that under the same axial and confining stress, the peak stress of the coal samples under axial stress

cyclic loading-unloading is lower than that under conventional loading. This may be due to the fatigue damage of coal caused by cyclic loading-unloading. Deformation reduces the strength of the coal samples, indicating that the loading path has a significant effect on the mechanical properties of coal.

3.2 Permeability of coal under axial stress cyclic loading and unloading

This experiment simulates the change in the gas seepage coefficient under the disturbance of cyclic load generated by outburst coal during the mining operation.

Through the gas flow rate recorded by the computer, the permeability is calculated according to Eq. (1). The percolation of gas in the coal in this experiment can be considered to obey Darcy's law:

$$K = \frac{2P_0'Q\,\mu L}{A(P_1^2 - P_2^2)} \quad (1)$$

where K is the permeability of the coal (mD), Q is the gas flow rate (ml/s), μ is the absolute viscosity of the gas, and the gas viscosity is 1.087×10-6 Pa·s at room temperature 20°C, P_0 is the standard atmospheric pressure, 0.101 MPa, P_1 is the inlet pressure (MPa), P_2 is the outlet pressure, where the standard atmospheric pressure is 0.101 MPa, A is the effective area of permeability (m^2), and L is the length of the coal sample (mm).

3.2.1 Effect of loading path on permeability

Rock unloading failure is a complicated process. Here, we only analyze the permeability changes during the axial stress cyclic loading-unloading stage. Fig. 4 shows the time course of the volumetric strain and permeability of the coal samples of specimen 1.

Notably, the permeability variation curve of coal and the volume strain variation curve have a clear symmetrical relationship. As the volume strain increases, the permeability decreases, and vice versa. With the unloading of the confining stress, the axial stress reaches the yield point, which causes damage to the specimen and a sharp increase in permeability.

Fig. 5 shows the results of the change in the permeability of specimen 1 during each loading-unloading cycle. In the initial stage of the test, the permeability of the coal first decreases rapidly and then slowly, which was caused by the existence of pore fractures. In the process of applying pressure, the original open structural plane and fractures gradually closed, the coal was compacted, and the gas flow channel became narrow. The permeability of the coal decreased with increasing stress, the axial stress reached the upper limit, and the permeability was reduced to a minimum. After entering the cyclic loading stages BC, CD, DE, and EF, the elastic deformation of the coal is continuously produced and recovered under the influence of axial compression . There is a negative correlation between coal permeability and axial stress. The changing path of coal permeability during each loading-unloading process is similar, but the amount of each change gradually decreases with the number of cycles. With the progress of the cycle,

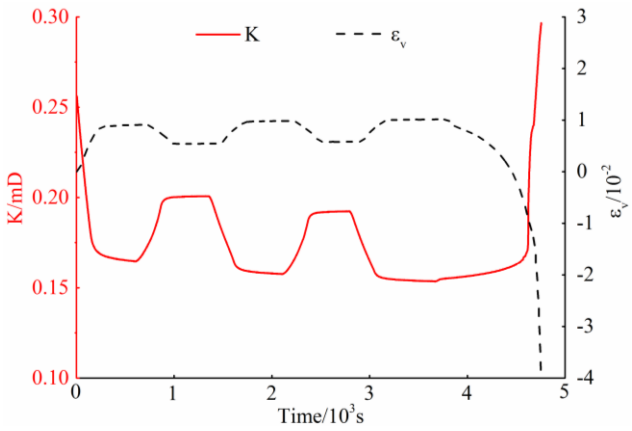

Fig. 4 Strain and permeability–time curves of specimen 1

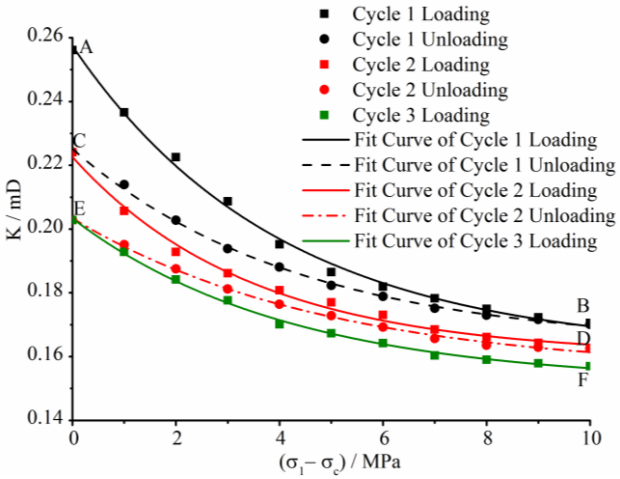

Fig. 5 Permeability results during cyclic loading-unloading conditions of Test 1

Table 1 Permeability fitting constants and R^2

Phase	Fitting constants			R^2
	A	B	C	
A-B	0.16155	0.09587	0.24912	0.99621
B-C	0.16342	0.06171	0.23036	0.99811
C-D	0.16031	0.06231	0.28949	0.99332
D-E	0.15518	0.04861	0.20543	0.99715
E-F	0.15169	0.05169	0.24039	0.99747

the elastic deformation of the coal cannot be completely recovered after the load is removed, i.e., some of the pores and fissures in the specimen are squeezed, which results in a certain plastic deformation and loss of coal permeability.

According to the results of Test 1 and research in the literature (Wang *et al.* 2012), Eq. (2) was used to regressively fit the experimental data to obtain the relationship between permeability and the principal stress difference index

$$k = A + B \times exp(-C \times \sigma_c) \quad (2)$$

where A, B, and C are all fitting constants.

Test 1 permeability variation of the fitting constants and

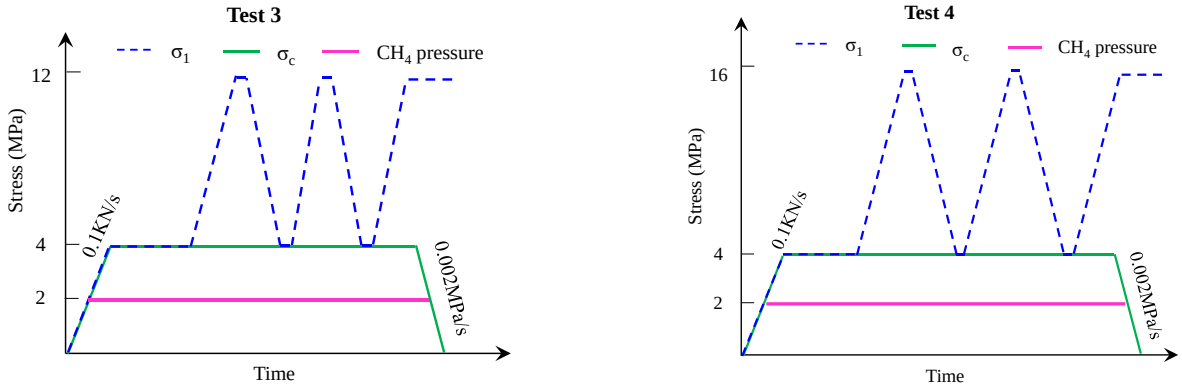

(a) Test 3 (b) Test 4

Fig. 6 Experimental scheme of the loading-unloading cycle under different peak axial stresses

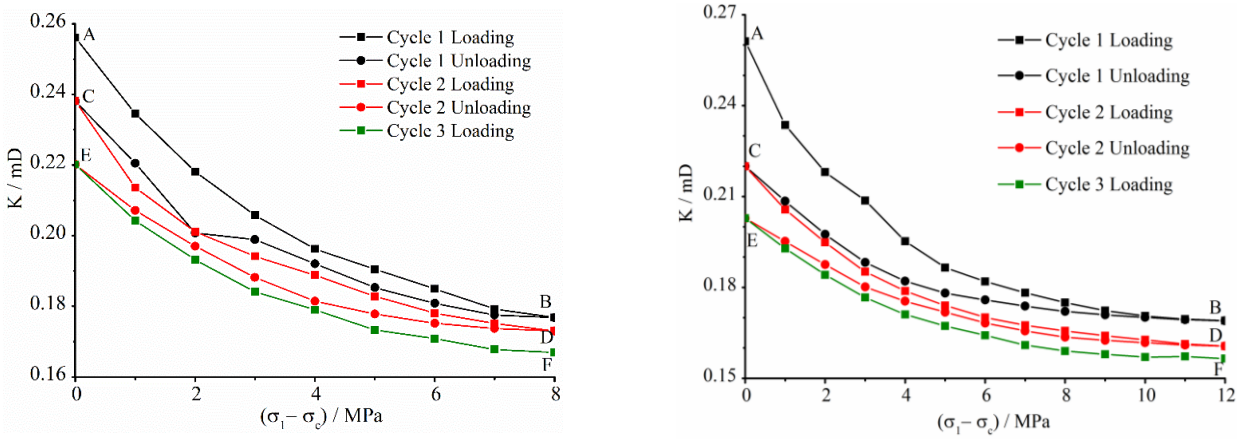

(a) Test 3 (12 MPa) (b) Test 4 (16 MPa)

Fig. 7 Coal permeability under different peak stresses as a function of principal stress difference

R^2 are as shown in Table 1. The greater the fit in this equation, the greater the ability to accurately characterize changes in permeability.

3.2.2 Effect of peak stress on permeability

According to statistics, coal mining in China has a wide range of mining depths, ranging from several hundred meters to thousands of meters (Du *et al*. 2019, 2020). Different coal mining depths will lead to different axial compression loads of coal seams. Owing to the inherent elastoplastic properties of coal/rocks, the peak axial compression will affect the mechanical properties of the material, leading to the expansion and closure of pores and fissures, affecting the permeability of coal seams. To study the effect of peak axial compression on permeability, two experimental schemes were designed based on Test 1, as shown in Fig. 6.

Fig. 7 shows the variation in permeability of the specimen with the difference in principal stress at different peak axial pressures. As shown in Figs. 6 and 8, taking the first cycle as an example, at a σ_1 of 12, 14, and 16 MPa, the permeability reduction values were 0.079, 0.087, and 0.090 mD, respectively, showing a positive correlation with σ_1. Although the permeability changes with the principal stress difference, it was similar in all three experimental groups; as σ_1 increases, the permeability at the corresponding point shows a decreasing trend. In each cycle, the minimum permeability in the peak stress state and the permeability recovery value when unloaded to hydrostatic pressure show a decreasing trend with the cycle periodicity. However, the change in permeability decreases with the number of cycles, and the range of change gradually decreases, indicating that the permeability is sensitive to stress.

The influence of axial stress on the coal pore-fracture structure and permeability characteristics is mainly reflected in the following three aspects: 1) As the axial stress increases, the effective stress on the coal increases, and the pore size in the coal matrix decreases, resulting in an increase in methane seepage resistance in the coal and a decrease in coal permeability. 2) As the axial stress increases, the effective stress on the coal increases, the opening degree of the coal fractures reduces, and some of the fractures close, resulting in a decrease in the seepage channels and permeability of the gas in the coal. 3) As the axial stress increases, the amount of coal adsorbed gas decreases, the corresponding adsorption expansion deformation decreases, the amount of fracture opening caused by adsorption expansion decreases, and the permeability increases (Liu *et al.* 2019). Therefore, the increase in axial stress has both a negative and positive

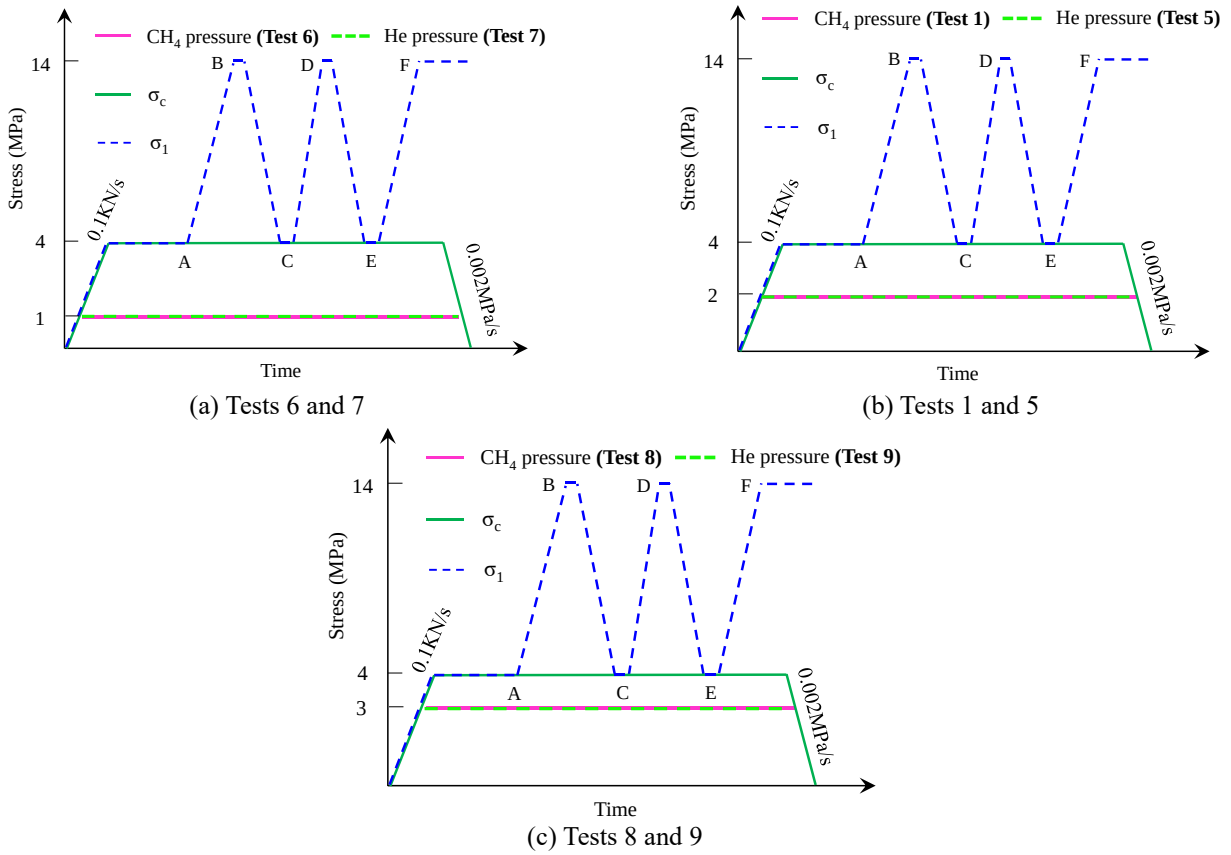

(a) Tests 6 and 7

(b) Tests 1 and 5

(c) Tests 8 and 9

Fig. 8 Experimental paths with various pore pressures

effect on the gas seepage process. The final change in permeability is the result of the competition between these two effects. It can be seen from Figs. 5 and 7 that permeability decreases with the increase in axial stress, indicating that the negative effect is more evident.

3.2.3 Effect of pore pressure on permeability

The conclusion that the permeability of porous media is related to pore pressure has been widely accepted. In recent years, the influence of adsorbed and non-adsorbed gases on the permeability of unconventional reservoirs has also been a research hotspot. In this experiment, constant external stress was set, and the pore methane pressure was set to 1, 2, and 3 MPa, and helium corresponding to the pore pressure was set for comparison experiments, as shown in Fig. 8.

Fig. 9 shows the variation in permeability with the principal stress difference under different pore pressure conditions. Overall, in each experiment, there was a negative correlation between permeability and principal stress difference. Moreover, regardless of the pore pressure, the permeability in the helium experiment was always greater than that in the methane experiment in the corresponding state.

Taking the first cycle of Tests 5 and 7 as examples, k_A is 0.81 and 0.96 mD, k_B is 0.34 and 0.40 mD, and k_C are 0.721 and 0.802 mD, respectively. Under the same stress state, in the helium medium, the permeability gradually increases with the increase in pore pressure. Taking the first cycle of the methane experiment as an example, at 1, 2, and 3 MPa, k_A is 0.286, 0.256, and 0.279 mD, k_B is 0.201, 0.171, and 0.189 mD, and k_C is 0.242, 0.224, and 0.241 mD, respectively.

As shown in Fig. 10, the permeability at various points in the methane environment and the irreversible permeability damage rate show a V-shape change. That is, the gas pressure is in the range of 1-2 MPa, which decreases with the increase in gas pressure, and the opposite is in the range of 2-3 MPa.

From the experimental results, the variation rules of coal permeability are clearly different. In the helium medium, because helium is a non-adsorbing gas, the coal matrix does not undergo expansion and deformation, and the coal matrix is only affected by the pore pressure F_1, except for the external pressure. When the external pressure is constant, owing to the increase in pore pressure, the decrease in effective stress changes the matrix strain and pore-fracture structure state inside the specimen, which increases the number of seepage channels and increases the seepage pore size, finally reflecting the increase in permeability 11(a).

As shown in Fig. 11(b), in the methane environment, the coal matrix is not only affected by the pore pressure F_1, but also by the expansion stress F_2 induced by the coal matrix adsorbing gas molecules (Wang *et al*. 2019a). The influence of gas pressure on the pore-fracture structure and permeability characteristics mainly includes the following three aspects. 1) The pore pressure increases, the effective stress on the coal matrix decreases, the pores become larger due to matrix relaxation, and the methane seepage resistance decreases, which increases permeability. 2) As

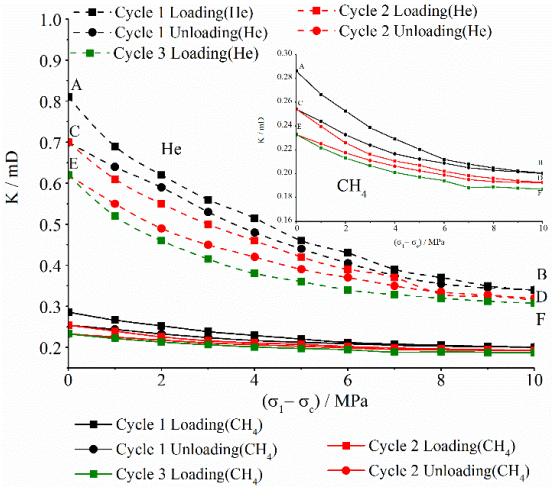

(a) Tests 6 and 7 (1 MPa)

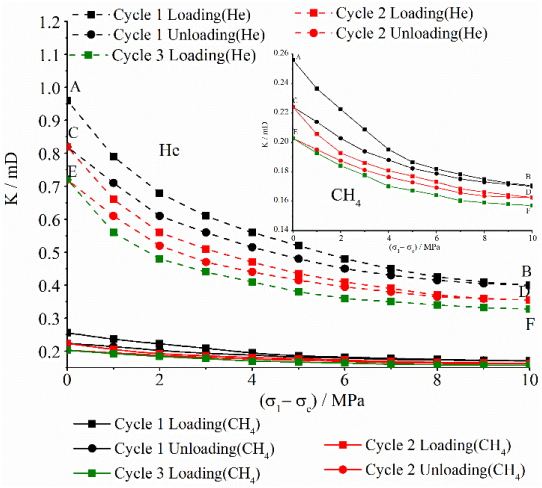

(b) Tests 1 and 5 (2 MPa)

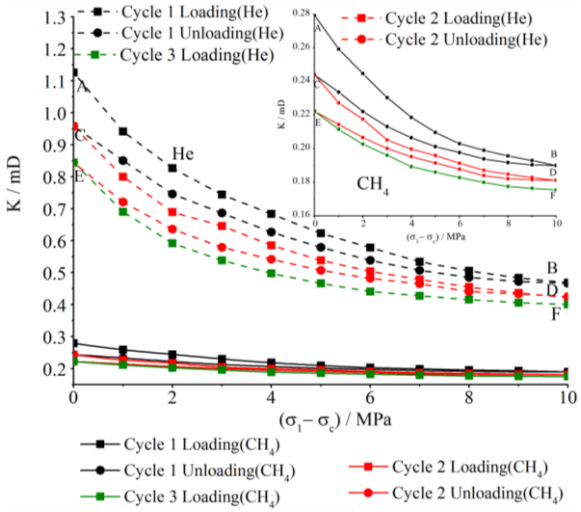

(c) Test 8 and 9 (3 MPa)

Fig. 9 Permeability results during cyclic loading conditions with pore pressure

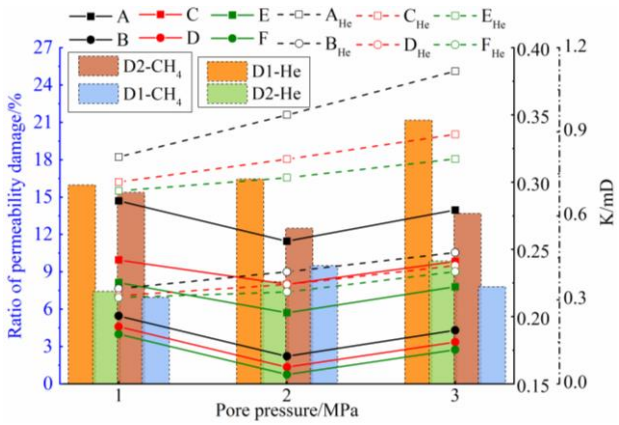

Fig. 10 Permeability damage influenced by pore pressure

the pore pressure increases, the effective stress on the coal matrix decreases, and the originally closed fractures inside the coal open. Concurrently, the original opening of the fractures increases, increasing the effective percolation channels of the gas and eventually leading to an increase in permeability. 3) With the increase in gas pressure, the expansion and deformation of the coal skeleton caused by the gas effect also increases, resulting in a decrease in the coal permeability volume, gas seepage velocity, and coal permeability (Liu *et al*. 2019). Therefore, the increase in gas pressure has both a positive and negative effect on seepage. The final change in permeability is the result of the competition between these two effects.

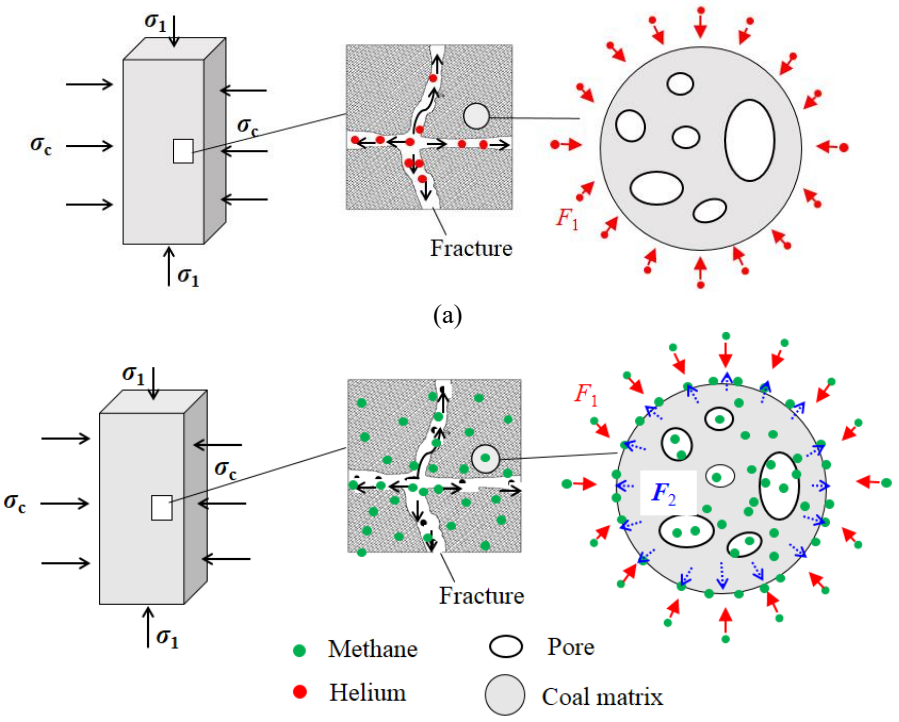

Fig. 11 Schematics showing testing with different gases; (a) helium and (b) methane

4. Discussion

4.1 Analysis of permeability damage

From the experimental results of the above groups, it can be seen that the permeability-principal stress difference curves do not coincide in each cycle, and the permeability is always smaller than the axial pressure loading phase during the axial pressure unloading phase. There is a significant difference in permeability during loading and unloading in the same stage. The value can represent the irreversible pore fractures and fissure changes generated by the coal sample during loading and unloading, i.e., irreversible permeability damage.

To quantitatively describe the degree of change in the permeability of coal samples, Jing (Wang *et al.* 2012) proposed the irreversible permeability damage rate of coal. The greater the irreversible permeability damage rate, the worse the recovery of coal sample permeability, which can be calculated using Eq. (3):

$$D_1 = \frac{k_A - k_C}{k_A} \times 100\% \quad (3)$$

where D_1 is the irreversible permeability damage rate of the first cycle of the coal sample, k_A is the coal sample permeability measured at point A, and k_C is the coal sample permeability measured at point C. Similarly, the irreversible permeability damage rate in the second cycle can be obtained.

Take the permeability values at each node in Tests 1, 3, and 4 and bring them into the above equation to obtain the effect of the peak axial stress on the rate of permeability loss, as shown in Fig. 8. After cyclic loading and unloading, the coal samples undergo irreversible plastic deformation, indicating that under the action of external pressure, the inherent pores and fissure structure of the coal change, causing a certain degree of permeability damage during each cycle of the loading-unloading process.

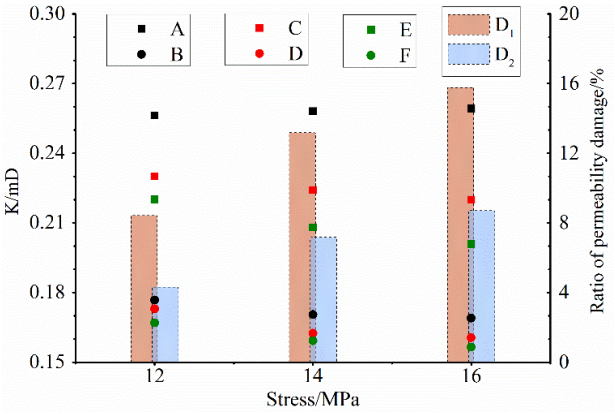

Fig. 12 Damage rate of permeability influenced by peak axial stress

As shown in Fig. 12, at 12, 14, and 16 MPa, the irreversible permeability damage rates in the first stage are 8.421, 13.180, and 15.777%, respectively, and the irreversible permeability damage rates in the second stage are 4.311, 7.184, and 8.713%, respectively. This phenomenon can also be observed in Fig. 10. Notably, the permeability damage amount and the axial pressure peak show a positive correlation, and the initial loading and unloading stage is the main stage of permeability damage to coal samples.

From the perspective of effective stress (Terzaghi, 1943), during the experiment, the axial and confining stresses are equivalent to the axial and the confining effective stresses. The increase in effective stress causes the coal sample to be compressed more densely, and the pore diameter of the coal molecules decreases. The smaller diameter reduces the effective percolation channel of methane, increases the resistance of gas molecules to movement, reduces the seepage speed of the methane, and ultimately results in a reduction in the permeability of the coal sample. Simultaneously, under these stress peaks, it is not enough to cause new fractures in the specimen; thus, the specimen does not appear damaged. Conversely, with the increase in axial stress, the pore fracture in the specimen is further compressed, resulting in a decrease in permeability. With the increase in the peak stresses, the damage rate of permeability gradually increases in the cyclic loading-unloading experiment, which again illustrates the sensitivity of permeability to stress.

4.2 Contribution of this experiment on dynamic disaster prevention and control

Under the disturbance of mining, the abutment stress of the coal in front of the working face is always in the dynamic change of strengthening and weakening, and the change in the pore/fracture structure causes fluctuations in the permeability of the coal.

In the initial stage of the influence of abutment stress, the stress is concentrated and the force acting on the coal gradually increases. However, because the degree of stress received is small and the failure limit is not reached, the coal is in the elastic compression stage, and the strain curve shows a monotonous downward trend. Under the action of stress, the original pores/fractures in the coal seam are compressed to varying degrees (or even closed) and the gas seepage channels are reduced. The result is that the gas permeability of the coal seam is reduced, the gas storage effect is more evident, and the pore pressure is greater. The increase in pore pressure harms coal permeability and is more conducive to the accumulation of coal seam methane. Under the dual effects of abutment stress and pore pressure, the coal permeability will be further reduced, and the strength of the coal sample will increase. At this time, coal and rock dynamic disaster accidents are prone to occur. When the abutment stress is weakened, as the stress is removed, the strain of the coal in an elastic state begins to recover. The pores/fractures originally in the compressed state expand and the permeability is recovered, but the strain value and permeability of the coal can be seen that none of them recovered to the initial value, and the permeability was lost every time the abutment stress was loaded and unloaded. Additionally, the permeability begins to increase, and the accumulated gas is immediately desorbed, leading to an acceleration of diffusion and seepage, conditions that favor coal and gas outburst disasters.

Currently, with the depletion of resources in Chinese shallow mines, mining is gradually expanding towards deeper wells. With deep mines, the phenomena of high stress and high pore pressure are more evident, and the superimposition of the phenomena will further increase the induction of dynamic disasters. Therefore, in the process of deep coal mining, in addition to conventional gas control measures, actions must be taken to relieve the abutment stress of the coal seam in front of the work face, eliminate the elastic potential energy of the coal, reduce the internal energy of the gas, and prevent the occurrence of coupled dynamic disasters such as rock bursts and gas outbursts.

5. Conclusions

Studying the influence of periodic pressure on coal seams in front of the working face can guide the prevention and control of the combined dynamic disasters of coal and gas outbursts and rock bursts. In this study, laboratory experiments of loading and unloading axial stress cycles were performed using briquettes, and the experimental parameters around the loading and unloading path, peak axial pressure, pore pressure, and pore medium were used. Based on this study, by comparing and analyzing the evolution of coal sample deformation, permeability change, and permeability irreversible damage rate, the following conclusions can be drawn.

1) There are obvious symmetrical relationship between the permeability curve of coal and the volumetric strain curve. In the process of axial pressure loading and unloading, the permeability of coal shows a negative power exponential function change. In the process of cyclic loading and unloading, the permeability can't recover to its initial value, which indicates that the permeability of coal will be damaged to a certain extent. The permeability difference and permeability damage decrease with the increase of cyclic loading and unloading times, and the change and damage of permeability mainly occur in the initial loading and unloading stage.

2) The strain-principal stress difference curves of the coal sample have "memory", and it will return to the original path after completing the cyclic loading and unloading of one stage and entering the next stage. The peak stress of coal samples under cyclic loading and unloading of axial compression is lower than that under conventional loading. Fatigue damage and deformation caused by cyclic loading and unloading path reduce the strength of coal samples. The permeability of coal containing gas decreases with the increase of axial pressure, and the permeability damage rate increases gradually, which indicates that permeability is sensitive to stress.

3) Under the same stress conditions, compared with helium environment, the permeability of coal samples in methane are always lower, and with the increase of gas pressure, the permeability shows a "V" shaped trend. This is due to the competitive effect of expansion deformation and shrinkage deformation caused by gas adsorption on coal matrix, which results in the change of pore-fracture structure in coal.

Declaration of competing interests

All authors declare that they have no conflicts of interest.

Acknowledgments

This research was financially supported by the National Natural Science Foundation of China (51874314, 51704187), the China Postdoctoral Science Foundation (2019M660861), and the Yue Qi Distinguished Scholar Project, China University of Mining & Technology Beijing, Shandong Province key research and development plan, China (2019GSF109068), the Key Laboratory of Mine Disaster Prevention and Control (Shandong University of Science and Technology) (MDPC202017).

References

Araei, A.A., Razeghi, H.R. and Ghalandarzadeh, A. (2012), "Effects of loading rate and initial stress state on stress-strain behavior of rock fill materials under monotonic and cyclicl loading conditions", *Sci. Iranica*, **19**, 1220-1235. http://doi.org/10.1016/j.scient.2012.08.002.

Chen, Y., Wang, S. and Wang, E. (2007), "Strength and elastic properties of sandstone under different testing conditions", *J. Central South Univ.*, **2**, 210-215. https://doi.org/10.1007/s11771-007-0042-z.

Du, F. and Wang, K. (2019), "Unstable failure of gas-bearing coal-rock combination bodies: Insights from physical experiments and numerical simulations", *Pro. Safe. Environ. Protect.*, **129**, 264-279. https://doi.org/10.1016/j.psep.2019.06.029.

Du, F., Wang, K. and Guo, Y. (2020), "The mechanism of rockburst-outburst coupling disaster considering the coal-rock combination: An experiment study", *Geomech. Eng.*, **22**(3), 255-264. https://doi.org/10.12989/gae.2020.22.3.255.

Elsworth, D., Wang, S. and Liu, J. (2012), "Mechanical behavior of methane infiltrated coal: The roles of gas desorption, stress level and loading rate", *Rock Mech. Rock. Eng.*, **46**(5), 945-958. https://doi.org/10.1007/s00603-012-0324-0.

Elsworth, D., Wang, S. and Liu, J. (2013), "Permeability evolution during progressive deformation of intact coal and implications for instability in underground coal seams", *Int. J. Rock Mech. Min. Sci.*, **58**, 34-45. https://doi.org/ 10.1016/j.ijrmms.2012.09.005.

Fan, L. and Liu, S. (2019), "Evaluation of permeability damage for stressed coal with cyclic loading: An experimental study", *Int. J. Coal Geol.*, **216**, 103338. https://doi.org/10.1016/j.coal.2019.103338.

Fuenkajorn, K. and Phueakphum, D. (2010), "Effects of cyclic loading on mechanical properties of Maha Sarakham salt", *Engg. Geol.*, **112**, 43-52. https://doi.org/10.1016/j.enggeo.2010.01.002.

Ghabezloo, S., Sulem, J. and Guedon, S. (2009), "Effective stress law for the permeability of a limestone", *Int. J. Rock Mech. Min. Sci.*, **46**(2), 297-306. https://doi.org/10.1016/j.ijrmms.2008.05.006.

Gordon, R.B. and Davis, L.A. (1967), "Velocity and attenuation of seismic waves in imperfectly elastic rock", *J. Geophys. Res.*, **73**(12), 3917-3935. https://doi.org/10.1029/JB073i012p03917.

Jafari, M.K., Pellet, F. and Boulon, M. (2004), "Experimental study of mechanical behaviour of rock joints under cyclic loading", *Rock Mech. Rock. Eng.*, **37**, 3-23. https://doi.org/10.1007/s00603-003-0001-4.

Jiang, F., Wu, H. and Guo, J. (2021), "Experimental study of the damage evolution and radon exhalation characteristics of quasi-uranium ore under constant amplitude cyclic loading and unloading", *J. Radioanal. Nucl. Chem.*, **327**(1), 373-384. https://doi.org/10.1007/S10967-020-07516-8.

Jorat, M.E., Kreiter, S. and Moerz, T. (2013), "Strength and compressibility characteristics of peat stabilized with sand columns", *Geomech. Eng.*, **5**(6), 575-594. https://doi.org/10.12989/gae.2013.5.6.575.

Kasani, H.A. and Chalaturnyk, R.J. (2017), "Influence of high pressure and temperature on the mechanical behavior and permeability of a fractured coal", *Energies*, **10**, 854. https://doi.org/10.3390/en1007085.

Lama, R. and Saghafi, A. (2002), Overview of gas outbursts and unusual emissions", *Proceedings of the 2002 Coal Operators' Conference*, Wollogong, Australia, February.

Li, Y., Zhang, S. and Zhang, B. (2018), "Dilatation characteristics of the coals with outburst proneness under cyclic loading conditions and the relevant applications", *Geomech. Eng.*, **14(**5), 459-466. http://doi.org/10.12989/gae.2018.14.5.459.

Liu, T. (2019), "Multifield coupling processes during gas drainage in deep fractured coal seam and its engineering response", Ph.D. Dissertation, China University of Mining and Technology, Beijing, China.

Martin, C., Kaiser, P. and Christiansson, R. (2003), "Stress, instability and design of underground excavations", *Int. J. Rock Mech. Min. Sci.*, **40**, 1027-1047. https://doi.org/10.1016/S1365-1609(03)00110-2.

Miao, S., Liu, Z. and Zhao, X. (2020), "Characteristics of energy dissipation and damage of Beishan granite under cyclic loading and unloading", *Chin. J. Rock Mech. Eng.*, https://doi.org/10.13722/j.cnki.jrme.2020.0953.

Mohamed, H.M. and Romao, X. (2018), "Performance analysis of a detailed FE modelling strategy to simulate the behaviour of masonry-infilled RC frames under cyclic loading", *Earthq. Struct.*, **14**(6), 551-565. http://doi.org/10.12989/eas.2018.14.6.551.

Rudakov, D. and Sobolev, V. (2019), "A mathematical model of gas flow during coal outburst initiation", *Int. J. Min. Sci.*, **29**(5), 791-796. https://doi.org/10.1016/j.ijmst.2019.02.002.

Russell, A., Shi, H. and Peter, M. (2004), "Influences of loading rate and preloading on the mechanical properties of dry elasto-plastic granules under compression", *Aichhe J.*, 1-14. https://doi.org/10.1002/aic.14572.

Sobczyk, J. (2011), "The influence of sorption processes on gas stresses leading to the coal and gas outburst in the laboratory conditions", *Fuel*, **90**(3), 1018-1023. https://doi.org/10.1016/j.fuel.2010.11.004.

Sobczyk, J. (2014), "A comparison of the influence of adsorbed gases on gas stresses leading to coal and gas outburst", *Fuel*, **115**, 288-294. https://doi.org/10.1016/j.fuel.2013.07.016.

Taheri, A., Hamzah, N. and Dai, Q. (2017), "Degradation and improvement of mechanical properties of rock under triaxial compressive cyclic loading", *Jap. Geotech. Soc. Sp. Pub.*, **5**(2), 71-78. https://doi.org/10.3208/jgssp.v05.017.

Terzaghi, K. (1943), Theoretical Soil Mechanics, John Wiley and Sons Inc., New York, U.S.A., 235-334.

Wang, D., Wei, J. and Yin, G. (2012), "Investigation on change rule of permeability of coal containing gas under complex stress paths", *Chin. J. Rock Mech. Eng.*, **31**(2), 303-310. https://doi.org/1000–6915(2012)02–0303–08.

Wang, G., Guo, Y., Du, C.A., Sun, L., Liu, Z., Wang, Y. and Cao, J (2019b), "Experimental study on damage and gas migration characteristics of gas-bearing coal with different pore structures under sorption-sudden unloading of methane", *Geofluids*, 1-11. https://doi.org/10.1155/2019/7287438.

Wang, G., Guo, Y., Wang, P., Li, W., Wu, M., Sun, L., Cao, J.J. and Du, C. (2019a), "A new experimental apparatus for sudden unloading of gas-bearing coal", *B. Eng. Geol. Environ.*, **79**, 857-868. https://doi.org/10.1007/s10064-019-01601-3.

Wang, K. and Du, F. (2019), "Experimental investigation on mechanical behavior and permeability evolution in coal-rock

combined body under unloading conditions", *Arab*. *J*. *Geosci*., **12**(14), 1-15. https://doi.org/ 10.1007/s12517-019-4582-y.

Wang, T., Wang, C. and Xue, F. (2021), "Acoustic emission characteristics and energy evolution of red sandstone samples under cyclic loading and unloading", *Shock Vib*. https://doi.org/10.1155/2021/8849137.

Wu, M., Wang, J. and Russell, A. (2020), "DEM modelling of mini-triaxial test based on one-to-one mapping of sand particles", *Géotechnique*, 1-14. https://doi.org/ 10.1680/jgeot.19.P.212.

Xie, J., Gao, M. and Zhang, R. (2020), "Gas flow characteristics of coal samples with different levels of fracture network complexity under triaxial loading and unloading conditions", *J*. *Petrol*. *Sci*. *Eng*., **195**, 107606. https://doi.org/10.1016/j.petrol.2020.107606.

Xu, J., Li, B. and Zhou, T. (2012), "Experimental study of deformation and seepage characteristics of coal under cyclic loading", *Chin*. *J*. *Rock Mech*. *Eng*., **33**(2), 225-234. https://doi.org/10.13722/j.cnki.jrme.2014.s2.021.

Zhang, B.J., Mei, C. and Huang, B. (2017), "Model tests on bearing capacity and accumulated settlement of a single pile in simulated soft rock under axial cyclic loading", *Geomech*. *Eng*., **12**(14), 611-626. http://doi.org/10.12989/gae.2017.12.4.611.

CC